

Noncentrosymmetric two-dimensional Weyl semimetals in porous Si/Ge structures

Emmanuel V. C. Lopes^a, Rogério J. Baierle^b, Roberto H. Miwa^a and Tome M. Schmidt^a

^aInstituto de Física, Universidade Federal de Uberlândia., Uberlândia, 38400-902, Minas Gerais, Brazil

^bDepartamento de Física, Universidade Federal de Santa Maria., Santa Maria, 97105-990, Rio Grande do Sul, Brazil

ARTICLE INFO

Keywords:

2D materials
Weyl semimetal
Topological materials
2D Porous structures
Si/Ge

ABSTRACT

In this work we predict a family of noncentrosymmetric two-dimensional (2D) Weyl semimetals composed by porous Ge and SiGe structures. These systems are energetically stable graphenylene-like structures with a buckling, spontaneously breaking the inversion symmetry. The nontrivial topological phase for these 2D systems occurs just below the Fermi level, resulting in nonvanishing Berry curvature around the Weyl nodes. The emerged Weyl semimetals are protected by C_3 symmetry, presenting one-dimensional edge Fermi-arcs connecting Weyl points with opposite chiralities. Our findings complete the family of Weyl in condensed-matter physics, by predicting the first noncentrosymmetric class of 2D Weyl semimetals.

1. Introduction

Among the materials with topological nontrivial phase, the Weyl semimetals (WSMs) are the last predicted [1–4] and experimentally observed ones [5–12]. This class of materials attracts attention by their interesting properties, such as chiral anomaly and negative magnetoresistance [13, 14]. They are potentially for applications in thermoelectricity, electronics, as well they present a connection with superconductivity, a subject in discussion [15–19]. WSMs are characterized by massless states in the bulk of the material with nonvanishing Chern number [20]. They are in pairs of opposite chirality nodes, where each crossing point is a singularity of the Berry curvature, presenting a monopole chiral charge [21]. The opposite chiral nodes in three-dimensional (3D) system present a bulk-boundary correspondence resulting in surface Fermi-arcs [22]. The 3D WSMs has been observed in many materials, where the Weyl nodes arise under breaking one of the fundamental symmetries, inversion [5–12] or time-reversal [2, 4, 23–25].

With the success and potential application of 3D WSMs, one should ask if a Weyl point would survive in a two-dimensional (2D) system. The possibility of 2D WSMs has been investigated using theoretical models [20, 26–28]. The fulfillment of 2D WSMs would be more promising for quantum computing and storage nanodevices due to the 2D architecture [29–31]. In 2D materials the Weyl points require extra symmetry protection, not needed in the counterpart 3D systems [20]. Recently it has been proposed WSMs in 2D systems such as MnNBr, Cr₂C, NiCS₃, CrN, VI₃, Mn₂NF₂, PtCl₃ and NpAs monolayers [32–39], all of them belonging to time-reversal symmetry breaking systems. For noncentrosymmetric systems, only quadratic Weyl semimetals have been proposed in a 2D heterostructure [40].

In this work, we predict noncentrosymmetric 2D WSMs protected by crystal symmetry in porous structures. The systems are similar to the graphenylene [41–43] but composed by Ge or SiGe. While graphenylene is planar sp²-carbon allotrope, the porous Ge and SiGe present a buckling, spontaneously breaking the inversion symmetry. The presence of topological nontrivial character just below the Fermi level, and the absence of inversion symmetry, are basic conditions to emerge pairs of Weyl nodes. Our results show that the Weyl nodes are protected by C_3 crystal symmetry, assuring their stability. The bulk-boundary correspondence is mediated by large energy dispersion edge arcs, connecting Weyl points with opposite chirality.

2. Methodology

Our calculations was based on first-principles within the density functional theory using the projector augmented waves method, implemented in Vienna *ab initio* simulation package (VASP) [44, 45]. The exchange-correlation term was described using the generalized gradient approximation (GGA) in Perdiew-Burke-Ernzehofer's (PBE) functional [46], including fully relativistic pseudopotentials. The plane wave basis set was used with a kinetic energy cut-off of 400 eV. To map the Brillouin zone it was used the Monkhost-Pack k-mesh grid of $11 \times 11 \times 1$. The topological properties such as Weyl chirality, Berry curvature, and projected edge states have been computed using the WannierTools package [47].

3. Results and discussion

The porous layered structures studied here are formed by squares connected to hexagons with large pores as shown in Fig. 1. The blue and magenta atoms can be either Si, Ge or both elements. All layers containing Si and/or Ge present a buckling degree, as shown in the figure, distinct from the centrosymmetric sp²-carbon graphenylene, which is planar [41, 42, 48]. The stability of these structures was confirmed through phonons calculations and *ab initio*

✉ emmanuelvictor96@gmail.com (E.V.C. Lopes); tschmidt@ufu.br (T.M. Schmidt)

ORCID(S): 0000-0002-7981-2161 (E.V.C. Lopes); 0000-0002-5948-1211 (R.J. Baierle); 0000-0002-1237-1525 (R.H. Miwa); 0000-0002-9121-8157 (T.M. Schmidt)

molecular dynamics simulations at finite temperatures [49]. Also the pores diameter of the Si/Ge structures are quite large, around 9 Å, as compared to the graphenylene porous around 6 Å [42], open it for new functionalities. The fully optimized lattice parameters were 10.60, 10.92 and 11.17 Å for Si, SiGe and Ge porous layers, respectively.

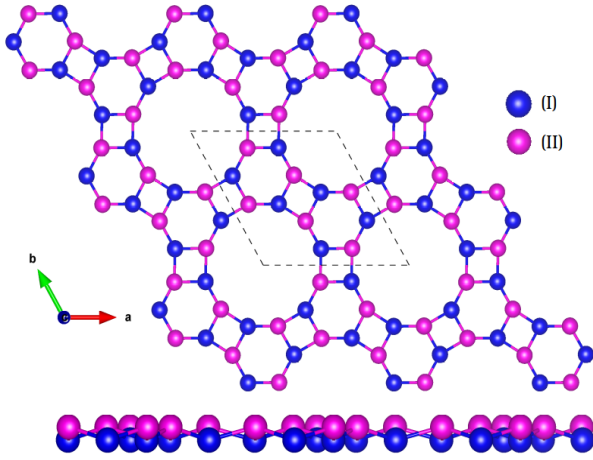


Figure 1: Top and side view of the crystal structure, showing the unit cell in dashed lines. Atoms (I) and (II) can be both Ge, or (I) Si and (II) Ge. Atom (I) is at lower position as compared to atom (II).

Our first-principles results shows that the porous structure of Si is metallic (not shown here). The SiGe and Ge structures present narrow band gap, as can be seen in Fig. 2. The band gap of the Ge comes from the spin-orbit coupling (SOC), without SOC it is metallic (Figs. 2(c-1) and 2(d-1)). A gap opening due to SOC is typically from topological nontrivial phase, as will be discussed below. The gapless for Si structure is due to its low SOC ($\lambda_{Si} = 3.9$ meV compared to $\lambda_{Ge} = 43$ meV [50]). For porous SiGe structure, due to the reduced symmetry, there is a band gap even without SOC, and the SOC effect splits the bands as can be seen in Figs. 2(a-2) and 2(b-1).

The band gaps are inverted for both SiGe and Ge structures at the Γ -point, similar to graphene. However, these porous systems present an additional inverted band, turning the whole system trivial with respect to the Fermi level. The second inversion is just below the top of valence band, leading to a couple of interesting band-crossings, emphasized in Figs. 2(a-3) and 2(c-3), for SiGe and Ge, respectively. Without SOC the bands are double degenerate, with massless Dirac-like crossings fourfold degenerated (Figs. 2(b-2) and 2(d-2)). The SOC split up the degeneracy, resulting pairs of nondegenerate bands crossing each other at two specific points. This is typically of Weyl semimetals, since the systems are noncentrosymmetric, but preserving time-reversal symmetry, as is required for a nonvanishing Berry curvature. For Si porous structure the low value of SOC parameter does not result in Weyl nodes.

In order to find the topological characteristic of a Dirac crossing, we compute the topological charge around each

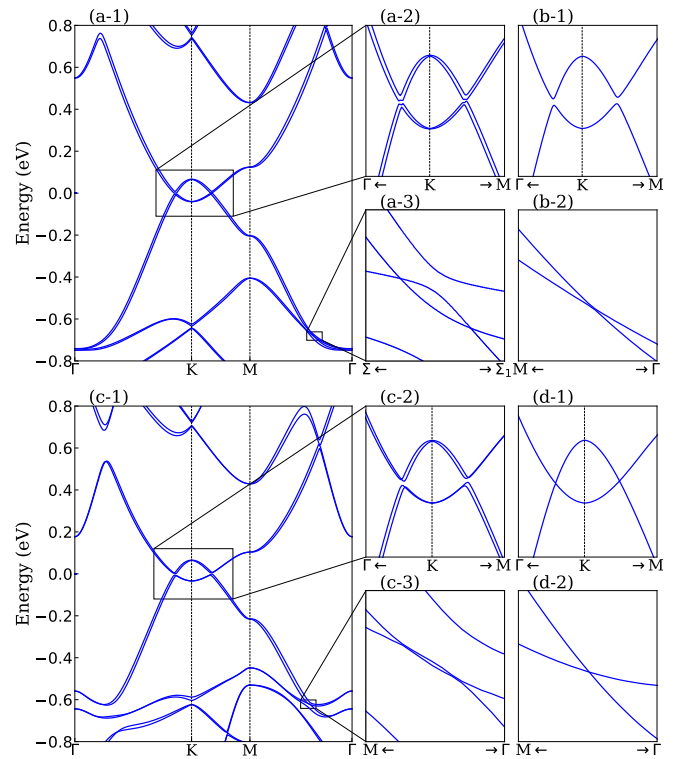


Figure 2: Band structure for porous SiGe (a)-(b) and Ge (c)-(d). The middle column are enlarged bands around the Fermi level and at the Weyl points. The last column are the same as the middle one, but without SOC.

crossing point. Starting from the Weyl equation [51], in Appendix A we derive an expression for the 2D Weyl chirality

$$\chi^{2D} = \frac{1}{\pi} \oint_l \mathbf{A}(\mathbf{k}) \cdot d\mathbf{k}. \quad (1)$$

Here $\mathbf{A}(\mathbf{k})$ corresponds to the Berry connection and l is a closed loop in momentum space around the supposed Weyl point. If nontrivial topological phase is present, each χ^{2D} carries ± 1 chirality value. By using the equation above our results shows that each crossing pair has the same chirality, but the all system is neutral, as can be seen in Fig. 3, in accordance with fermion doubling theorem [52, 53]. Weyl pairs with the same chirality are less common, but have been reported in 3D materials, such as magnetic-doped $\text{Sn}_{1-x}\text{Pb}_x(\text{Se}, \text{Te})$, $\text{AgBi}(\text{Cr}_2\text{O}_7)_2$ [24, 25] and, in the 2D Cr_2C monolayer [33]. As Ge and SiGe structures belong to a distinct space group symmetries, P_{622} (or D_6^1) and P_6 (or C_6^1), respectively, the 2D Weyl nodes are located at similar positions but at different directions. While the pair of Weyl nodes for germanylene are along the high-symmetry Γ -M direction, the low symmetric SiGe Weyl crossings are just out of the Γ -M direction, $\Sigma - \Sigma_1$ path as represented by green line in Fig. 3(a). Both systems present a total of six pairs of Weyl crossings protected by crystal symmetry, as is required for 2D WSMs [20], here the C_3 rotation symmetry.

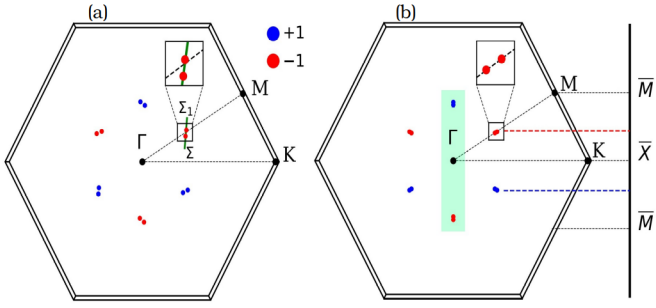


Figure 3: Weyl point chiralities on the 2D Brillouin zone for porous SiGe (a) and Ge (b). Inset of each figure is a zoom around the nodes to illustrate the splitting of Weyl pairs with the same chirality. The red circles corresponds to negative chirality and blue circles positive chirality.

The Berry curvature for a 2D Weyl system, as deduced in Appendix A, is aligned perpendicular to the xy -plane formed by a delta function centered at the Dirac crossing point k_0 of the Brillouin zone (BZ)

$$\Omega_{k_0}^{2D} = \pm\pi\delta^2(\mathbf{k} - \mathbf{k}_0)\mathbf{e}_z. \quad (2)$$

We compute the Berry curvature for germanylene using the DFT results projected onto the Wannier orbital basis. Fig. 4 shows the Berry curvature for a region in the BZ containing two pairs of Weyl points (rectangular dashed region marked in Fig. 3(b)). The computed Berry curvature from our first-principles calculation is a didactic result, showing delta functions centered at each Weyl point (inset of Fig. 4 is a better resolution, showing the splitting of $\chi^{2D} = -1$ chirality pair). These results are in concordance with the Berry curvature property for time-reversal symmetry protected crystals $\Omega(\mathbf{k}) = -\Omega(-\mathbf{k})$ [20].

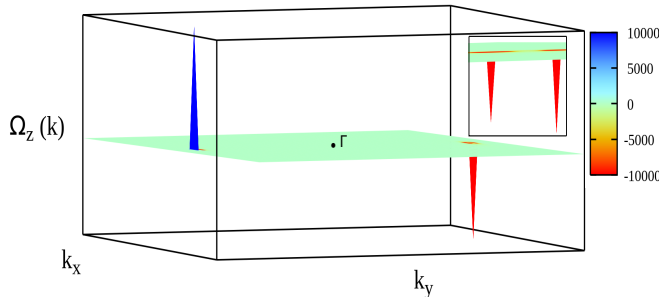


Figure 4: Computed Berry curvature for porous Ge structure. The $k_x k_y$ -plane corresponds to the aquamarine rectangle marked in Fig. 3(b). The inset is a zoom showing the split of Weyl pairs with negative chirality.

One of the main characteristic of topological materials is the bulk-boundary correspondence. In the class of 3D WSMs, this correspondence is expressed by surface states that connects Weyl points with opposite chiralities, the Fermi-arcs. In 2D materials, the presence of Weyl nodes inside the 2D bulk, induces edge states restricted to just one momentum direction. These edge Fermi-arcs can be visualized by performing a band structure calculation of a ribbon.

In Figs. 5(a) and 5(b) it can be seen the projected edge bands that connects Weyl nodes with opposite chiralities for SiGe and Ge porous structures, respectively. There are two edge states connecting two pairs of Weyl nodes, projected along a k -line perpendicular to the Γ - K direction (see Fig. 3(b)). Although the spin of the Fermi-arc bands is lifted, there is not net magnetization in the system, due to the preservation of the time-reversal symmetry. It is worth to note that the edge arcs present large energy dispersions, a characteristic also observed in 2D WSMs where time-reversal symmetry is broken [32, 33, 37].

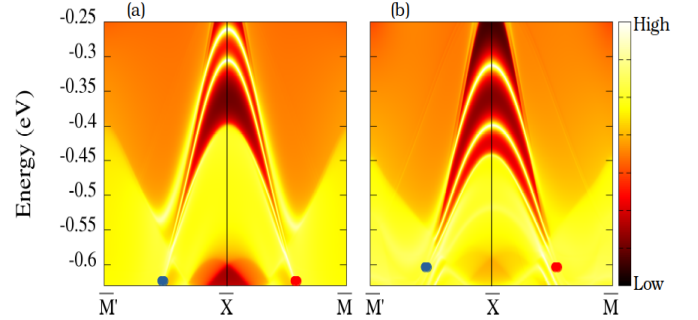


Figure 5: Projected 1D edge states connecting Weyl points with opposite chirality for porous SiGe (a) and Ge (b) ribbons. The edge $\bar{M}' - \bar{X} - \bar{M}$ path is illustrated in Fig. 3-(b).

4. Conclusion

In summary, based on topological invariant calculations and first-principles results, we propose a family of noncentrosymmetric 2D WSMs. It is a porous structure, similar to the graphenylene, but composed by Ge or SiGe. The structure presents a buckling, spontaneously breaking the inversion symmetry. By computing the Weyl chirality in both systems, we identify six pairs of Weyl nodes protected by C_3 crystal symmetry. The computed 1D edge Fermi-arc shows large energy dispersion connecting Weyl points with opposite chiralities. Our findings complete the family of Weyls in condensed-matter physics, by predicting the first noncentrosymmetric class of 2D WSMs.

Note

During the revision process to submit this article, an arXiv preprint [54] was uploaded, reporting the first experimental verification of a 2D Weyl semimetal observed in epitaxial bismuthene. Those findings corroborate our results, demonstrating the feasibility of 2D WSMs.

Acknowledgments

The authors acknowledge Brazilian agencies FAPEMIG, CAPES, CNPq and INCT-Nanocarbono for financial support. Also Laboratório Nacional de Computação Científica (LNCC-SCAFMat2) and CENAPAD-SP for the computational resources.

A. Two-dimensional Weyl Chirality

The Hamiltonian proposed by Weyl [51] can be used for crossing points in condensed matter physics, by including a velocity v_F for the fermions in the form [55]

$$H = \hbar v_F \mathbf{k} \cdot \boldsymbol{\sigma}. \quad (3)$$

Here $\boldsymbol{\sigma}$ corresponds to the Pauli's matrix and \mathbf{k} the crystal momentum. The isotropic 2D Weyl Hamiltonian in the xy -plane can be written as

$$H = \hbar v_F (k_x \sigma_x + k_y \sigma_y). \quad (4)$$

The solution of Schrödinger's equation for the Eq. 4 Hamiltonian, gives the eigenvalues $\epsilon = \pm \hbar v_F k$, with $k = \sqrt{(k_x^2 + k_y^2)}$. Using the more appropriate cylindrical coordinates, the respective eigenfunctions are given by

$$\psi_{\pm \hbar v_F k} = \frac{1}{\sqrt{2}} \begin{pmatrix} \pm e^{-i\theta} \\ 1 \end{pmatrix}, \quad (5)$$

with positive (negative) exponential term for positive (negative) momentum eigenvalue.

In order to compute a topological variable associated to a Weyl point, like a chiral charge, we start from the Berry phase [56]. The corresponding Berry connection can be computed from the eigenfunctions above

$$\mathbf{A}(\mathbf{k}) = i \langle \psi_{\pm} | \nabla_{\mathbf{k}} | \psi_{\pm} \rangle, \quad (6)$$

where $\nabla_{\mathbf{k}}$ is the gradient operator. The Berry connection for each momentum eigenvalue is then given by

$$\mathbf{A}(\mathbf{k}) = \pm \frac{1}{2k} \mathbf{e}_{\theta}. \quad (7)$$

For 3D systems the chiral topological charge is computed by the Berry flux over a 2D closed Fermi surface around the Weyl node. While for a 2D system, the Berry flux can be obtained by integrated over a closed Fermi ring around the Weyl node

$$\varphi = \oint_l \mathbf{A}(\mathbf{k}) \cdot d\mathbf{k}. \quad (8)$$

By using the derived Berry connection (Eq. 7), the integral gives a nonvanishing flux $\varphi = \pm\pi$. In this way we can define a topological variable associated with the Weyl chirality of a 2D system, by the expression

$$\chi = \frac{1}{\pi} \oint_l \mathbf{A}(\mathbf{k}) \cdot d\mathbf{k} = \pm 1. \quad (9)$$

Another characteristic of Weyl physics can be derived from the Berry curvature, which is given by the curl of Berry connection, $\boldsymbol{\Omega} = \nabla \times \mathbf{A}$. It can be noted, by taken the curl in cylindrical coordinates, that the Berry curvature is null for $k \neq 0$. In the limit that \mathbf{k} tends to zero, we have a divergence, which means that, in this case, the Berry curvature is a delta function

$$\boldsymbol{\Omega} = \pm \pi \delta^2(\mathbf{k}) \mathbf{e}_z. \quad (10)$$

Applying the Stokes' theorem to the Berry curvature of Eq. 10, integrating over the 2D BZ, results in $\chi = \pm 1$, the same as Eq. 9 for the chirality of 2D Weyls.

References

- [1] S. Murakami, Phase transition between the quantum spin hall and insulator phases in 3d: emergence of a topological gapless phase, *New Journal of Physics* 10 (2) (2008) 029802. doi:10.1088/1367-2630/10/2/029802.
- [2] X. Wan, A. M. Turner, A. Vishwanath, S. Y. Savrasov, Topological semimetal and fermi-arc surface states in the electronic structure of pyrochlore iridates, *Phys. Rev. B* 83 (2011) 205101. doi:10.1103/PhysRevB.83.205101.
- [3] A. A. Burkov, L. Balents, Weyl semimetal in a topological insulator multilayer, *Phys. Rev. Lett.* 107 (2011) 127205. doi:10.1103/PhysRevLett.107.127205.
- [4] K.-Y. Yang, Y.-M. Lu, Y. Ran, Quantum hall effects in a weyl semimetal: Possible application in pyrochlore iridates, *Phys. Rev. B* 84 (2011) 075129. doi:10.1103/PhysRevB.84.075129.
- [5] B. Q. Lv, N. Xu, H. M. Weng, J. Z. Ma, P. Richard, X. C. Huang, L. X. Zhao, G. F. Chen, C. E. Matt, F. Bisti, V. N. Strocov, J. Mesot, Z. Fang, X. Dai, T. Qian, M. Shi, H. Ding, Observation of weyl nodes in TaAs, *Nature Physics* 11 (9) (2015) 724–727. doi:10.1038/nphys3426.
- [6] S.-Y. Xu, I. Belopolski, D. S. Sanchez, C. Zhang, G. Chang, C. Guo, G. Bian, Z. Yuan, H. Lu, T.-R. Chang, P. P. Shibayev, M. L. Prokopovych, N. Alidoust, H. Zheng, C.-C. Lee, S.-M. Huang, R. Sankar, F. Chou, C.-H. Hsu, H.-T. Jeng, A. Bansil, T. Neupert, V. N. Strocov, H. Lin, S. Jia, M. Z. Hasan, Experimental discovery of a topological weyl semimetal state in tap, *Science Advances* 1 (10) (2015) e1501092. doi:10.1126/sciadv.1501092.
- [7] S.-Y. Xu, I. Belopolski, N. Alidoust, M. Neupane, G. Bian, C. Zhang, R. Sankar, G. Chang, Z. Yuan, C.-C. Lee, S.-M. Huang, H. Zheng, J. Ma, D. S. Sanchez, B. Wang, A. Bansil, F. Chou, P. P. Shibayev, H. Lin, S. Jia, M. Z. Hasan, Discovery of a weyl fermion semimetal and topological fermi arcs, *Science* 349 (6248) (2015) 613–617. doi:10.1126/science.aaa9297.
- [8] S.-M. Huang, S.-Y. Xu, I. Belopolski, C.-C. Lee, G. Chang, B. Wang, N. Alidoust, G. Bian, M. Neupane, C. Zhang, S. Jia, A. Bansil, H. Lin, M. Z. Hasan, A weyl fermion semimetal with surface fermi arcs in the transition metal monopnictide TaAs class, *Nature Communications* 6 (1) (jun 2015). doi:10.1038/ncomms8373.
- [9] H. Weng, C. Fang, Z. Fang, B. A. Bernevig, X. Dai, Weyl semimetal phase in noncentrosymmetric transition-metal monophosphides, *Phys. Rev. X* 5 (2015) 011029. doi:10.1103/PhysRevX.5.011029.
- [10] L. Lu, Z. Wang, D. Ye, L. Ran, L. Fu, J. D. Joannopoulos, M. Soljačić, Experimental observation of weyl points, *Science* 349 (6248) (2015) 622–624. doi:10.1126/science.aaa9273.
- [11] S.-Y. Xu, N. Alidoust, I. Belopolski, Z. Yuan, G. Bian, T.-R. Chang, H. Zheng, V. N. Strocov, D. S. Sanchez, G. Chang, C. Zhang, D. Mou, Y. Wu, L. Huang, C.-C. Lee, S.-M. Huang, B. Wang, A. Bansil, H.-T. Jeng, T. Neupert, A. Kaminski, H. Lin, S. Jia, M. Z. Hasan, Discovery of a weyl fermion state with fermi arcs in niobium arsenide, *Nature Physics* 11 (9) (2015) 748–754. doi:10.1038/nphys3437.
- [12] N. Xu, H. M. Weng, B. Q. Lv, C. E. Matt, J. Park, F. Bisti, V. N. Strocov, D. Gawryluk, E. Pomjakushina, K. Conder, N. C. Plumb, M. Radovic, G. Autès, O. V. Yazyev, Z. Fang, X. Dai, T. Qian, J. Mesot, H. Ding, M. Shi, Observation of weyl nodes and fermi arcs in tantalum phosphide, *Nature Communications* 7 (1) (mar 2016). doi:10.1038/ncomms11006.
- [13] D. T. Son, B. Z. Spivak, Chiral anomaly and classical negative magnetoresistance of weyl metals, *Phys. Rev. B* 88 (2013) 104412. doi:10.1103/PhysRevB.88.104412.
- [14] A. A. Zyuzin, A. A. Burkov, Topological response in weyl semimetals and the chiral anomaly, *Phys. Rev. B* 86 (2012) 115133. doi:10.1103/PhysRevB.86.115133.
- [15] P. O. Sukhachov, E. V. Gorbar, Superconductivity in weyl semimetals in a strong pseudomagnetic field, *Phys. Rev. B* 102 (2020) 014513. doi:10.1103/PhysRevB.102.014513.
- [16] F. Han, N. Andrejevic, T. Nguyen, V. Kozii, Q. T. Nguyen, T. Hogan, Z. Ding, R. Pablo-Pedro, S. Parjan, B. Skinner, A. Alatas, E. Alp,

- S. Chi, J. Fernandez-Baca, S. Huang, L. Fu, M. Li, Quantized thermoelectric hall effect induces giant power factor in a topological semimetal, *Nature Communications* 11 (1) (dec 2020). doi:10.1038/s41467-020-19850-2.
- [17] V. Arjona, M. N. Chernodub, M. A. H. Vozmediano, Fingerprints of the conformal anomaly in the thermoelectric transport in dirac and weyl semimetals, *Phys. Rev. B* 99 (2019) 235123. doi:10.1103/PhysRevB.99.235123.
- [18] C. Fu, S. N. Guin, T. Scaffidi, Y. Sun, R. Saha, S. J. Watzman, A. K. Srivastava, G. Li, W. Schnelle, S. S. P. Parkin, C. Felser, J. Gooth, Largely suppressed magneto-thermal conductivity and enhanced magneto-thermoelectric properties in ptn, *Research* 2020 (2020) 1–8. doi:10.34133/2020/4643507.
- [19] P.-F. Liu, J. Li, C. Zhang, X.-H. Tu, J. Zhang, P. Zhang, B.-T. Wang, D. J. Singh, Type-ii dirac cones and electron-phonon interaction in monolayer biphenylene from first-principles calculations, *Phys. Rev. B* 104 (2021) 235422. doi:10.1103/PhysRevB.104.235422.
- [20] S. A. Yang, Dirac and weyl materials: Fundamental aspects and some spintronics applications, *SPIN* 06 (02) (2016) 1640003. doi:10.1142/S2010324716400038.
- [21] N. P. Armitage, E. J. Mele, A. Vishwanath, Weyl and dirac semimetals in three-dimensional solids, *Rev. Mod. Phys.* 90 (2018) 015001. doi:10.1103/RevModPhys.90.015001.
- [22] B. Q. Lv, T. Qian, H. Ding, Experimental perspective on three-dimensional topological semimetals, *Rev. Mod. Phys.* 93 (2021) 025002. doi:10.1103/RevModPhys.93.025002.
- [23] J. Ruan, S.-K. Jian, D. Zhang, H. Yao, H. Zhang, S.-C. Zhang, D. Xing, Ideal weyl semimetals in the chalcopyrites CuTe_2 , AgTe_2 , AuTe_2 , and ZnPtAs_2 , *Phys. Rev. Lett.* 116 (2016) 226801. doi:10.1103/PhysRevLett.116.226801.
- [24] G. Chang, B. J. Wieder, F. Schindler, D. S. Sanchez, I. Belopolski, S.-M. Huang, B. Zhang, D. Wu, T.-R. Chang, T. Neupert, S.-Y. Xu, H. Lin, M. Z. Hasan, Topological quantum properties of chiral crystals, *Nature Materials* 17 (11) (2018) 978–985. doi:10.1038/s41563-018-0169-3.
- [25] J. Liu, C. Fang, L. Fu, Tunableweyl fermions and fermi arcs in magnetized topological crystalline insulators*, *Chinese Physics B* 28 (4) (2019) 047301. doi:10.1088/1674-1056/28/4/047301.
- [26] Y. Guo, Z. Lin, J.-Q. Zhao, J. Lou, Y. Chen, Two-dimensional tunable dirac/weyl semimetal in non-abelian gauge field, *Scientific Reports* 9 (1) (dec 2019). doi:10.1038/s41598-019-54670-5.
- [27] H. Isobe, N. Nagaosa, Coulomb interaction effect in weyl fermions with tilted energy dispersion in two dimensions, *Phys. Rev. Lett.* 116 (2016) 116803. doi:10.1103/PhysRevLett.116.116803.
- [28] L. Hao, C. S. Ting, Topological phase transitions and a two-dimensional weyl superconductor in a half-metal/superconductor heterostructure, *Phys. Rev. B* 94 (2016) 134513. doi:10.1103/PhysRevB.94.134513.
- [29] S. Bader, S. Parkin, Spintronics, *Annual Review of Condensed Matter Physics* 1 (1) (2010) 71–88. doi:10.1146/annurev-conmatphys-070909-104123.
- [30] X. Li, X. Wu, Two-dimensional monolayer designs for spintronics applications, *WIREs Computational Molecular Science* 6 (4) (2016) 441–455. doi:https://doi.org/10.1002/wcms.1259.
- [31] D. D. Awschalom, M. E. Flatté, Challenges for semiconductor spintronics, *Nature Physics* 3 (3) (2007) 153–159. doi:10.1038/nphys551.
- [32] Y. Shi, L. Li, X. Cui, T. Song, Z. Liu, MnBr monolayer: A high-temperature ferromagnetic half-metal with type-ii weyl fermions, *Physica Status Solidi (RRL) – Rapid Research Letters* 15 (7) (2021) 2100115. doi:https://doi.org/10.1002/pssr.202100115.
- [33] W. Meng, X. Zhang, Y. Liu, L. Wang, X. Dai, G. Liu, Two-dimensional weyl semimetal with coexisting fully spin-polarized type-i and type-ii weyl points, *Applied Surface Science* 540 (2021) 148318. doi:https://doi.org/10.1016/j.apsusc.2020.148318.
- [34] G.-G. Li, R.-R. Xie, L.-J. Ding, W.-X. Ji, S.-S. Li, C.-W. Zhang, P. Li, P.-J. Wang, Two-dimensional weyl semi-half-metallic nics3 with a band structure controllable by the direction of magnetization, *Phys. Chem. Chem. Phys.* 23 (2021) 12068–12074. doi:10.1039/D1CP00812A.
- [35] T. He, X. Zhang, Y. Liu, X. Dai, G. Liu, Z.-M. Yu, Y. Yao, Ferromagnetic hybrid nodal loop and switchable type-i and type-ii weyl fermions in two dimensions, *Phys. Rev. B* 102 (2020) 075133. doi:10.1103/PhysRevB.102.075133.
- [36] T. Jia, W. Meng, H. Zhang, C. Liu, X. Dai, X. Zhang, G. Liu, Weyl fermions in vi3 monolayer, *Frontiers in Chemistry* 8 (2020). doi:10.3389/fchem.2020.00722.
- [37] X.-P. Wei, N. Yang, J. Shen, X. Tao, Ferromagnetic weyl semimetals and quantum anomalous hall effect in 2d half-metallic mn2nt2, *Physica E: Low-dimensional Systems and Nanostructures* 140 (2022) 115164. doi:https://doi.org/10.1016/j.physe.2022.115164.
- [38] J.-Y. You, C. Chen, Z. Zhang, X.-L. Sheng, S. A. Yang, G. Su, Two-dimensional weyl half-semimetal and tunable quantum anomalous hall effect, *Phys. Rev. B* 100 (2019) 064408. doi:10.1103/PhysRevB.100.064408.
- [39] X. Zou, N. Mao, B. Li, W. Sun, B. Huang, Y. Dai, C. Niu, Antiferromagnetic topological crystalline insulator and mixed weyl semimetal in two-dimensional npas monolayer, *New Journal of Physics* 23 (12) (2021) 123018. doi:10.1088/1367-2630/ac3cf5.
- [40] X. Zhao, F. Ma, P.-J. Guo, Z.-Y. Lu, Two-dimensional quadratic double weyl semimetal, *Phys. Rev. Res.* 4 (2022) 043183. doi:10.1103/PhysRevResearch.4.043183.
- [41] Q. Song, B. Wang, K. Deng, X. Feng, M. Wagner, J. D. Gale, K. Müllen, L. Zhi, Graphenylene, a unique two-dimensional carbon network with nonlocalized cyclohexatriene units, *J. Mater. Chem. C* 1 (2013) 38–41. doi:10.1039/C2TC00006G.
- [42] Q.-S. Du, P.-D. Tang, H.-L. Huang, F.-L. Du, K. Huang, N.-Z. Xie, S.-Y. Long, Y.-M. Li, J.-S. Qiu, R.-B. Huang, A new type of two-dimensional carbon crystal prepared from 1,3,5-trihydroxybenzene, *Scientific Reports* 7 (1) (jan 2017). doi:10.1038/srep40796.
- [43] G. Brunetto, P. A. S. Autreto, L. D. Machado, B. I. Santos, R. P. B. dos Santos, D. S. Galvão, Nonzero gap two-dimensional carbon allotrope from porous graphene, *The Journal of Physical Chemistry C* 116 (23) (2012) 12810–12813. doi:10.1021/jp211300n.
- [44] G. Kresse, J. Hafner, *abinitio* molecular dynamics for liquid metals, *Physical Review B* 47 (1) (1993) 558–561. doi:10.1103/physrevb.47.558.
- [45] G. Kresse, J. Furthmüller, Efficient iterative schemes for ab initio total-energy calculations using a plane-wave basis set, *Phys. Rev. B* 54 (1996) 11169–11186. doi:10.1103/PhysRevB.54.11169.
- [46] J. P. Perdew, K. Burke, M. Ernzerhof, Generalized gradient approximation made simple, *Physical Review Letters* 77 (18) (1996) 3865–3868. doi:10.1103/physrevlett.77.3865.
- [47] Q. Wu, S. Zhang, H.-F. Song, M. Troyer, A. A. Soluyanov, Wanniertools : An open-source software package for novel topological materials, *Computer Physics Communications* 224 (2018) 405 – 416. doi:https://doi.org/10.1016/j.cpc.2017.09.033.
- [48] R. M. Meftakhutdinov, R. T. Sibatov, A. I. Kochaev, Graphenylene nanoribbons: electronic, optical and thermoelectric properties from first-principles calculations, *Journal of Physics: Condensed Matter* 32 (34) (2020) 345301. doi:10.1088/1361-648X/ab8a9f.
- [49] L. F. Kremer, R. J. Baierle, Stability, electronic and optical properties of group iv graphenylene-like materials. an ab initio investigation, *Manuscript submitted for publication* (2023).
- [50] C.-C. Liu, H. Jiang, Y. Yao, Low-energy effective hamiltonian involving spin-orbit coupling in silicene and two-dimensional germanium and tin, *Phys. Rev. B* 84 (2011) 195430. doi:10.1103/PhysRevB.84.195430.
- [51] H. Weyl, GRAVITATION AND THE ELECTRON, *Proceedings of the National Academy of Sciences* 15 (4) (1929) 323–334. doi:10.1073/pnas.15.4.323.
- [52] H. Nielsen, M. Ninomiya, The adler-bell-jackiw anomaly and weyl fermions in a crystal, *Physics Letters B* 130 (6) (1983) 389–396. doi:https://doi.org/10.1016/0370-2693(83)91529-0.
- [53] H. Nielsen, M. Ninomiya, Absence of neutrinos on a lattice: (i). proof by homotopy theory, *Nuclear Physics B* 185 (1) (1981) 20–40. doi:https://doi.org/10.1016/0550-3213(81)90361-8.

- [54] Q. Lu, P. V. S. Reddy, H. Jeon, A. R. Mazza, M. Brahlek, W. Wu, S. A. Yang, J. Cook, C. Conner, X. Zhang, A. Chakraborty, Y.-T. Yao, H.-J. Tien, C.-H. Tseng, P.-Y. Yang, S.-W. Lien, H. Lin, T.-C. Chiang, G. Vignale, A.-P. Li, T.-R. Chang, R. G. Moore, G. Bian, Observation of 2d weyl fermion states in epitaxial bismuthene, arXiv preprint arXiv:2303.02971 (2023). doi:10.48550/arXiv.2303.02971.
- [55] A. Burkov, Weyl metals, Annual Review of Condensed Matter Physics 9 (1) (2018) 359–378. doi:10.1146/annurev-conmatphys-033117-054129.
- [56] M. V. Berry, Quantal phase factors accompanying adiabatic changes, Proceedings of the Royal Society of London. A. Mathematical and Physical Sciences 392 (1802) (1984) 45–57. doi:10.1098/rspa.1984.0023.